supporting Information

An Effective Strategy to Achieve Excellent Energy Storage Properties in Lead-Free $BaTiO_3$ Based Bulk Ceramics

Zhonghua Dai[1,*], Jinglong Xie [1], Weiguo Liu [1*], Xi Wang[2], Lin Zhang [3], Zhijian Zhou [4], Jinglei Li [3], and Xiaobing Ren [4,5]

[1]Shaanxi Province Key Laboratory of Thin Films Technology & Optical Test, Xi'an Technological University, Xi'an 710032, China

[2]Key Laboratory of Luminescence and Optical Information Ministry of Education School of Science, Beijing Jiaotong University, Beijing 100044, China

[3]Electronic Materials Research Laboratory, Key Laboratory of the Ministry of Education & International Center for Dielectric Research, School of Electronic Science and Engineering, Faculty of Electronic and Information Engineering, Xi'an Jiaotong University, Xi'an 710049, China

[4]Frontier Institute of Science and Technology, and State Key Laboratory for Mechanical Behavior of Materials, Xi'an Jiaotong University, Xi'an 710049, China

[5]Center for Function Materials, National Institute for Materials Science, Tsukuba 3050047, Ibaraki, Japan

*Corresponding Authors: zhdai@mail.xjtu.edu.cn; wgliu@163.com.

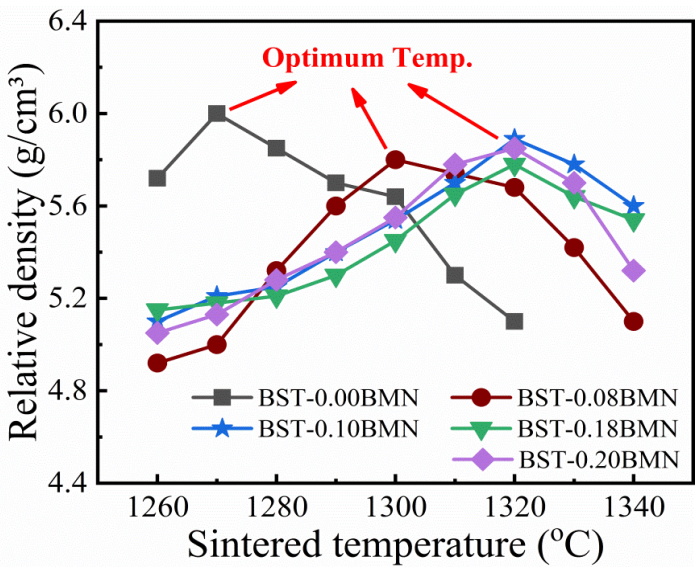

Figure S1. The density of BST-*x*BMN ceramics as a function of sintered temperature for 300 min (the density value of ceramics were measured by Archimedes method).

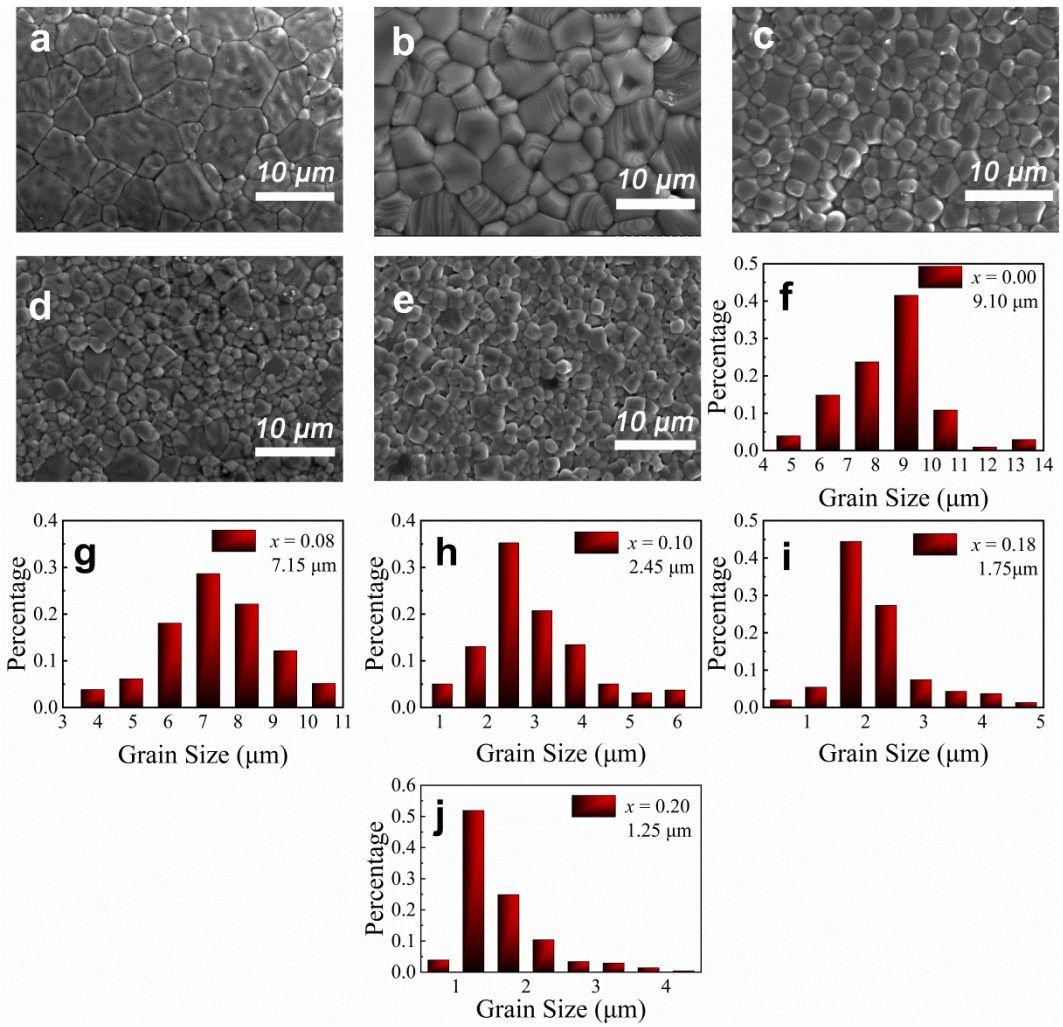

Figure S2. SEM micrographs on the original surfaces of the BST-*x*BMN ceramics (a) *x*=0.00,

(b) x=0.08, (c) x=0.10, (d) x=0.18, (e) x=0.20; and (f)-(j) average grain size of the various x.

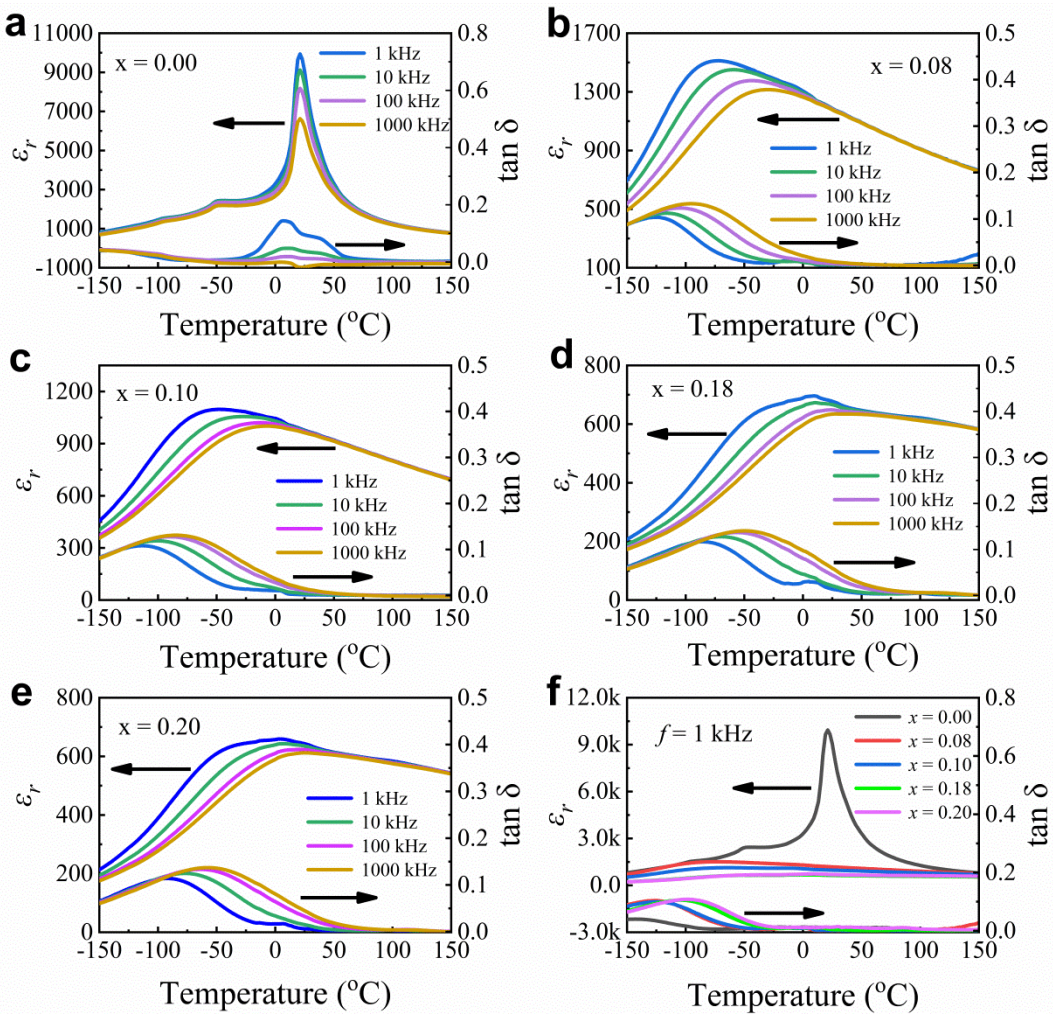

Figure S3. Temperature (-150 °C to 150 °C) dependence of dielectric permittivity and dielectric loss of BST-xBMN ceramics measured from 1 kHz to 1000 kHz, (a) x=0.00, (b) x=0.08, (c) x=0.10, (d) x=0.18, (e) x=0.20; (f) Temperature (-150 °C to 150 °C) dependence of dielectric permittivity and dielectric loss of BST-xBMN ceramics measured at 1 kHz.

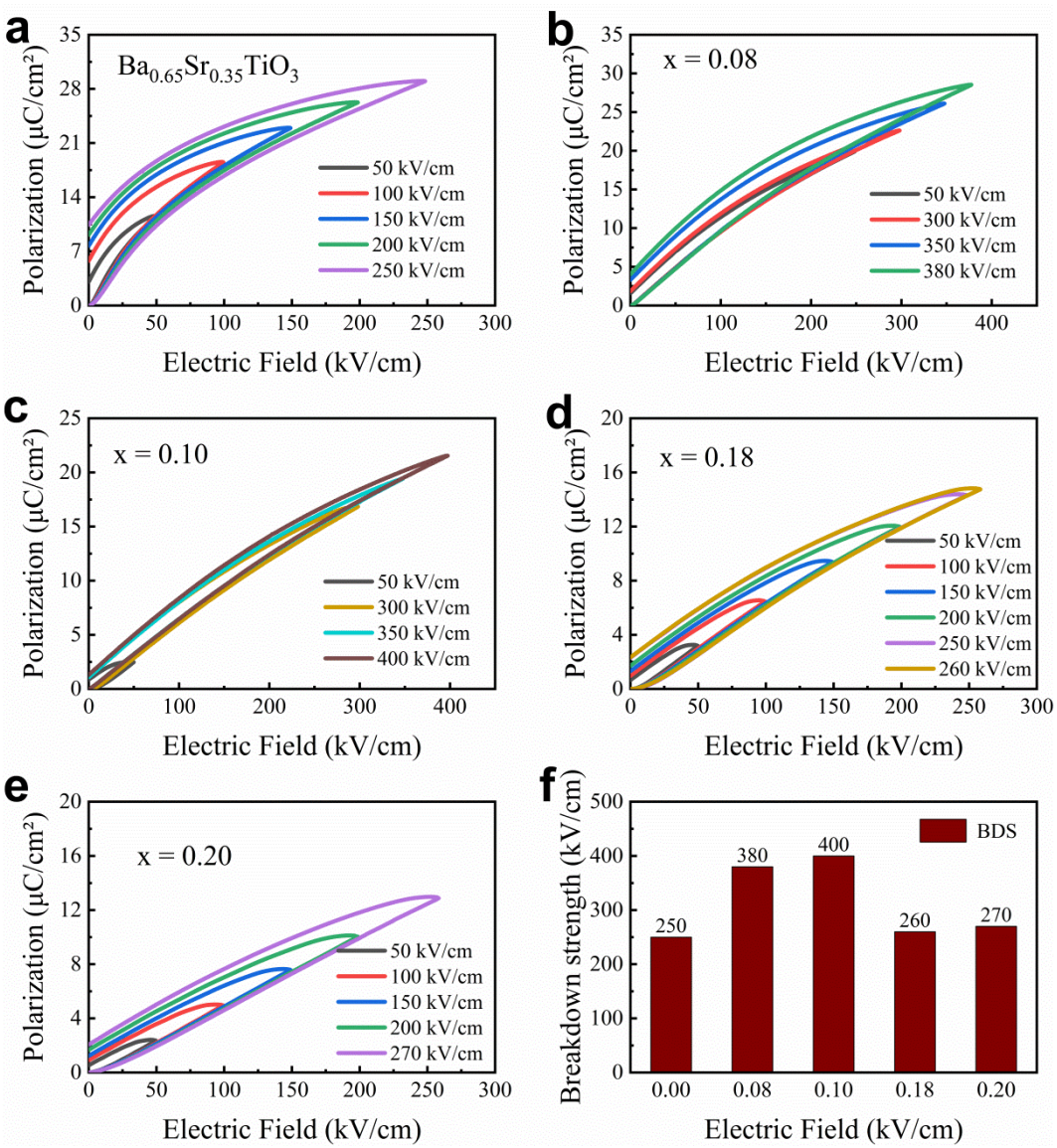

Figure S4. *P-E* loops measured under different electric fields at 10 Hz for BST-*x*BMN ceramics, (a) *x*=0.00, (b) *x*=0.08, (c) *x*=0.10, (d) *x*=0.18, (e) *x*=0.20; (f) breakdown strength (BDS) of BST-*x*BMN ceramics.

Table S1. Energy storage properties reported for lead free dielectric ceramics.

Materials	BDS ($kV \cdot cm^{-1}$)	ε_r	Tan δ	W ($J \cdot cm^{-3}$)	$Wrec$ ($J \cdot cm^{-3}$)	η (%)	Ref.
$BaTiO_3$-0.10$Bi(Mg_{2/3}Nb_{1/3})O_3$	140	1509	0.022	1.18	1.13	95.7	[1]
$BaTiO_3$-0.09$BiYbO_3$	93	-	-	0.86	0.71	82.6	[2]
$BaTiO_3$-0.10$Bi(Zn_{0.5}Zr_{0.5})O_3$	264	1900	0.024	-	2.46	-	[3]
$BaTiO_3$-0.15$Bi(Mg_{0.5}Zr_{0.5})O_3$	185	900	0.015	1.31	1.25	95.4	[4]
$BaTiO_3$-0.12$Bi(Mg_{0.5}Ti_{0.5})O_3$	224	1560	0.018	2.06	1.81	88	[5]
$BaTiO_3$-0.08$K_{0.73}Bi_{0.09}NbO_3$	327	2900	-	2.89	2.51	86.89	[6]
$BaTiO_3$-0.12$Bi(Li_{0.5}Nb_{0.5})O_3$	270	1180	0.01	2.31	2.03	88	[7]
$BaTiO_3$-0.12$Bi(Ni_{2/3}Nb_{1/3})O_3$	200	1266	0.004	2.18	2.09	95.9	[8]
$Ba_{0.5}Sr_{0.5}Ti_{0.997}Mn_{0.003}O_3$	290	2190	0.003	1.87	1.69	90.4	[9]
$(Bi_{0.85}Nd_{0.15})FeO_3-0.25BaTiO_3$	170	-	-	4.1	1.82	41.3	[10]
$Bi_{0.83}Sm_{0.17}Fe_{0.95}Sc_{0.05}O_3$	230	-	-	2.91	2.21	76	[11]
0.62$BiFeO_3$-0.3$BaTiO_3$ -0.08$Nd(Mg_{2/3}Nb_{1/3})O_3$	240	-	-	3.40	2.45	72	[12]
0.61$BiFeO_3$-0.33$BaTiO_3$ -0.06$La(Mg_{0.5}Ti_{0.5})O_3$	130	-	-	2.02	1.66	82	[13]
0.65$BiFeO_3$-0.3$BaTiO_3$-0.05Bi $(Zn_{2/3}Nb_{1/3})O_3$+0.1wt%Mn_2O_3	180	600	0.005	3.7	2.06	53	[14]
(0.75$Bi_{0.5}Na_{0.5}TiO_3$-0.25$Bi_{0.5}K_{0.5}$ TiO_3)-0.06$BiAlO_3$	105	-	-	1.57	1.15	73.2	[15]
0.92$Bi_{0.5}Na_{0.5}TiO_3$-0.06Ba TiO_3-0.2$SrTi_{0.875}Nb_{0.1}O_3$	105	2300	0.07	1.29	1.17	91	[16]
0.92(0.35$Bi_{0.5}Na_{0.5}TiO_3$-0.65Ba TiO_3)-0.08$Na_{0.73}Bi_{0.09}NbO_3$	172	2050	0.05	2.07	1.70	82	[17]
$(Ba_{0.06}Bi_{0.47}Na_{0.47})_{0.98}La_{0.02}Ti_{0.96}Zr_{0.04}O_3$	136	2130	0.04	2.14	1.55	72.6	[18]
$Bi_{0.5}Na_{0.5}TiO_3$-0.5$SrTiO_3$-3wt% MgO	227	2400	0.045	4.34	2.17	50	[19]
$(K_{0.5}Na_{0.5})NbO_3$-0.2$Sr(Sc_{0.5}Nb_{0.5})O_3$-0.5 mol% ZnO	400	-	-	3.55	2.6	73.2	[20]
$NaNbO_3$-0.10$Bi(Mg_{2/3}Nb_{1/3})O_3$	300	825	0.023	3.4	2.8	82	[21]
$NaNbO_3$-0.20$SrTiO_3$	310	1450	0.002	3.74	3.02	80.7	[22]
$NaNbO_3$-0.07$Bi(Mg_{0.5}Zr_{0.5})O_3$	255	1270	0.024	2.88	2.31	80.2	[23]
$Ba_{0.65}Sr_{0.35}TiO_3$-0.10$Bi(Mg_{2/3}Nb_{1/3})O_3$	400	1040	0.016	3.90	3.34	85.71	This work

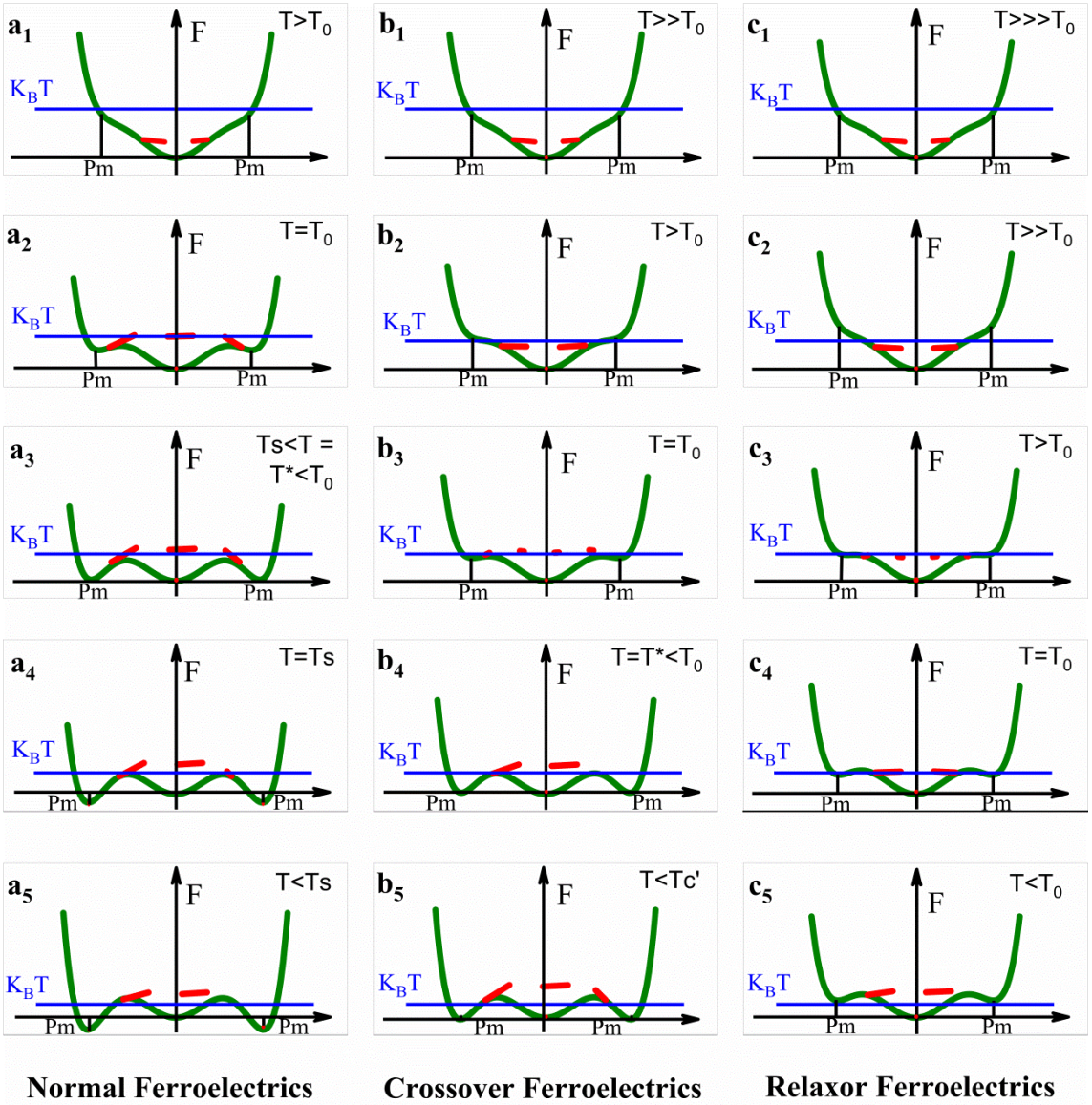

Figure S5. A phenomenological model for the doped relaxor system.

Landau Theory. The model system considered is a generic ferroelectric ceramic undergoing a first-order cubic-to-tetragonal ferroelectric transition upon cooling. The total free energy of the system includes the following three physically distinctive terms:

$$F = F(\mathbf{P},\bar{c}) + F(\mathbf{P},\varphi) + F(\mathbf{P}) = \int_V f_{bulk} dV + \int_V f_{couple} dV + \int_V (f_{elas} + f_{elec} + f_{grad}) dV$$

where V is the system volume, f_{bulk} denotes the Landau bulk free-energy density, f_{couple} denotes the free-energy density of the local polarization field, f_{elsa} is the elastic energy density, f_{elec} is the electrostatic energy density and f_{grad} is the gradient energy density.

The first term describing the global transition temperature effect (GTTE) and the bulk free energy density can be expressed by a Landau polynomial:

$$f_{bulk} = A_1 \sum_{i=1,2,3} P_i^2 + A_{11} \sum_{i=1,2,3} P_i^4 + \frac{A_{12}}{2} \sum_{i,j=1,2,3;i\neq j} (P_iP_j)^2 + A_{111} \sum_{i=1,2,3} P_i^6 + A_{112} \sum_{i,j=1,2,3;i\neq j} (P_iP_j)^4 + A_{123}(P_1^2P_2^2P_3^3)$$

where A_1, A_{11}, A_{12}, A_{111}, A_{112}, and A_{123} are the dielectric stiffness and higher-order stiffness coefficients.

The f_{couple} describes the local field effect (LFE), which can be expressed by Landau theory:

$$f_{couple} = -\int d^3x \sum_{i}^{3} P_i(\mathrm{x}) \cdot \varphi_{loc}(\mathrm{x})$$

where $\varphi_{loc}(\mathrm{x})$ is a random vector field created by the point defects.

Reference

[1] Wang, T.; Jin, L.; Li, C. C.; Hu, Q. Y.; Wei, X. Y. Relaxor Ferroelectric $BaTiO_3$-$Bi(Mg_{2/3}Nb_{1/3})O_3$ Ceramics for Energy Storage Application. *J. Am. Ceram. Soc.* **2014**, *98*, 559-566.

[2] Shen, Z. B.; Wang, X. H.; Luo, B. C.; Li, L. T. $BaTiO_3$-$BiYbO_3$ Perovskite Materials for Energy Storage Applications. *J. Mater. Chem. A* **2015**, *3*, 18146-18153.

[3] Yuan, Q. B.; Yao, F. Z.; Wang, Y. F.; Ma, R.; Wang, H. Relaxor Ferroelectric $0.9BaTiO_3$–$0.1Bi(Zn_{0.5}Zr_{0.5})O_3$ Ceramic Capacitors with High Energy Density and Temperature Stable Energy Storage Properties. *J. Mater. Chem. C* **2017**, *5*, 9552-9558.

[4] Jiang, X. W.; Hao, H.; Zhang, S. J.; Lv, J. H.; Cao, M. H.; Yao, F. Z.; Liu, H. X. Enhanced Energy Storage and Fast Discharge Properties of $BaTiO_3$ Based Ceramics Modified by $Bi(Mg_{1/2}Zr_{1/2})O_3$. *J. Eur. Ceram. Soc.* **2019**, *39*, 1103-1109.

[5] Hu, Q. Y.; Jin, L.; Wang, T.; Li, C. C.; Xing, Z.; Wei, X. Y. Dielectric and Temperature Stable Energy Storage Properties of $0.88BaTiO_3$-$0.12Bi(Mg_{1/2}Ti_{1/2})O_3$ Bulk Ceramics. *J. Alloys Compd.* **2015**, *640*, 416-420.

[6] Lin, Y.; Li, D.; Zhang, M.; Zhan, S. L.; Yang, Y. D.; Yang, H. B.; Yuan, Q. B. Excellent Energy-Storage Properties Achieved in $BaTiO_3$-Based Lead-Free Relaxor Ferroelectric Ceramics via Domain Engineering on the Nanoscale. *ACS Appl. Mater. Interfaces* **2019**, *11*, 36824-36830.

[7] Li, W. B.; Zhou, D.; Pang, L. X.; Xu, R.; Guo, H. Novel Barium Titanate Based

Capacitors with High Energy Density and Fast Discharge Performance. *J. Mater. Chem. A* **2017**, *5*, 19607-19612.

[8] Zhou, M. X.; Liang, R. H.; Zhou, Z.; Dong, X. L. Combining High Energy Efficiency and Fast Charge-Discharge Capability in Novel $BaTiO_3$-Based Relaxor Ferroelectric Ceramic for Energy-Storage. *Ceram. Int.* **2019**, *45*, 3582-3590.

[9] Huang Y. H.; Liu, B.; Liu, X. Q.; Li, J.; Wu, Y. J. Defect Dipoles Induced High-Energy Storage Density in Mn-Doped BST Ceramics Prepared by Spark Plasma Sintering. *J. Am. Ceram. Soc.* **2019**, *102*, 1904-1911.

[10] Wang, D. W.; Fan, Z. M.; Zhou, D.; Khesro, A.; Murakami, S.; Feteira, A.; Zhao, Q. L.; Tan, X. L.; Reaney. I. M. Bismuth Ferrite-Based Lead-Free Ceramics and Multilayers with High Recoverable Energy Density. *J. Mater. Chem. A* **2018**, *6*, 4133-4144.

[11] Gao, X. L.; Li, Y.; Chen, J. W.; Yuan, C.; Zeng, M.; Zhang, A. H.; Gao, X. S.; Lu, X. B.; Li, Q. L.; Liu, J. M. High Energy Storage Performances of $Bi_{1-x}Sm_xFe_{0.95}Sc_{0.05}O_3$ Lead-Free Ceramics Synthesized by Rapid Hot Press Sintering. *J. Eur. Ceram. Soc.* **2019**, *39*, 2331-2338.

[12] Wang, G.; Li, J. L.; Zhang, X.; Fan, Z. M.; Yang, F.; Feteira, A.; Zhou, D.; Sinclair, D.; Ma, T.; Tan, X. L.; Wang, D. W.; Reaney, I. M. Ultrahigh Energy Storage Density Lead-Free Multilayers by Controlled Electrical Homogeneity. *Energy. Environ. Sci.* **2019**, *12*, 582-588.

[13] Zheng, D. G.; Zuo, R. Z. Enhanced Energy Storage Properties in $La(Mg_{1/2}Ti_{1/2})O_3$-Modified $BiFeO_3$-$BaTiO_3$ Lead-Free Relaxor Ferroelectric Ceramics Within a Wide Temperature Range. *J. Eur. Ceram. Soc.* **2017**, *37*, 413-418.

[14] Wang, D. W.; Fan, Z. M.; Li, W. B.; Zhou, D.; Feteira, A.; Wang, G.; Murakami, S.; Sun, S. K.; Zhao, Q. L.; Tan, X. L.; Reaney, I. M. High Energy Storage Density and Large Strain in $Bi(Zn_{2/3}Nb_{1/3})O_3$-Doped $BiFeO_3$-$BaTiO_3$ Ceramics. *ACS Appl. Energy Mater.* **2018**, *1*, 4403-4412.

[15] Yu, Z. L.; Liu, Y. F.; Shen, M. Y.; Qian, H.; Li, F. F.; Lyu, Y. N. Enhanced Energy Storage Properties of $BiAlO_3$ Modified $Bi_{0.5}Na_{0.5}TiO_3$–$Bi_{0.5}K_{0.5}TiO_3$ Lead-Free Antiferroelectric Ceramics. *Ceram. Int.* **2017**, *43*, 7653-7659.

[16] Shi, J.; Liu, X.; Tian, W. C. High Energy-Storage Properties of $Bi_{0.5}Na_{0.5}TiO_3$-$BaTiO_3$-$SrTi_{0.875}Nb_{0.1}O_3$ Lead-Free Relaxor Ferroelectrics. *J. Mater. Sci. Techno.* **2018**, *34*, 2371-2374.

[17] Yang, H. B.; Yan, F.; Lin, Y.; Wang, T.; Wang, F.; Wang, Y. L.; Guo, L. N.; Tai, W. D.; Wei, H. Lead-Free $BaTiO_3$-$Bi_{0.5}Na_{0.5}TiO_3$-$Na_{0.73}Bi_{0.09}NbO_3$ Relaxor Ferroelectric

Ceramics for High Energy Storage. *J. Eur. Ceram. Soc.* **2017**, *37*, 3303-3311.

[18] Wang, H.; Hu, Q.; Liu, X. Q.; Zheng, Q. J.; Jiang, N.; Yang, Y.; Kwok, K. W.; Xu, C. G.; Lin, D. M. A High-Tolerance BNT-Based Ceramic with Excellent Energy Storage Properties and Fatigue/Frequency/Thermal Stability. *Ceram. Int.* **2019**, *45*, 23233-23240.

[19] Huang, N.; Liu, H. X.; Hao, H.; Yao, Z. H.; Cao, M. H.; Xie, J. Energy Storage Properties of MgO-Doped $0.5Bi_{0\cdot5}Na_{0\cdot5}TiO_3$-$0.5SrTiO_3$ Ceramics. *Ceram. Int.* **2019**, *45*, 14921-14927.

[20] Qu, B. Y.; Du, H. L.; Yang, Z. T.; Liu, Q. H.; Liu, T. H. Enhanced Dielectric Breakdown Strength and Energy Storage Density in Lead-Free Relaxor Ferroelectric Ceramics Prepared Using Transition Liquid Phase Sintering. *RSC Adv.* **2016**, *6*, 34381-34389.

[21] Ye, J. M.; Wang, G. S.; Zhou, M. X.; Liu, N. T.; Chen, X. F.; Li, S.; Cao, F.; Dong, X. L. Excellent Comprehensive Energy Storage Properties of Novel Lead-Free $NaNbO_3$-Based Ceramics for Dielectric Capacitor Applications. *J. Mater. Chem. C* **2019**, *7*, 5639-5645.

[22] Zhou, M. X.; Liang, R. H.; Zhou, Z. Y.; Yan, S. G.; Dong, X. L. Novel Sodium Niobate-Based Lead-Free Ceramics as New Environment-Friendly Energy Storage Materials with High Energy Density, High Power Density, and Excellent Stability. *ACS Sustainable Chem. Eng.* **2018**, *6*, 12755-12765.

[23] Qu, N.; Du, H. L.; Hao, X. H. A New Strategy to Realize High Comprehensive Energy Storage Properties in Lead-Free Bulk Ceramics. *J. Mater. Chem. C* **2019**, *7*, 7993-8002.

[24] Wang, D.; Ke, X. Q.; Wang, Y. Z.; Gao, J. H.; Wang, Y.; Zhang, L. X.; Yang, S.; Ren, X. B. Phase Diagram of Polar States in Doped Ferroelectric Systems. *Phys. Rev. B* **2012**, *86*, No. 054120.

[25] Li, F.; Lin, D. B.; Chen, Z. B.; Cheng, Z. X.; Wang, J. L.; Li, C. C.; Xu, Z.; Huang, Q. W.; Liao, X. Z.; Chen, L. Q.; Shrout, T. R.; Zhang, S. J. Ultrahigh Piezoelectricity in Ferroelectric Ceramics By Design. *Nature Mater.* **2018**, *17*, 349-354.